Available online at www.sciencedirect.com
ScienceDirect
Trans. Nonferrous Met. Soc. China 33(2023) 1452−1459
Transactions of Nonferrous Metals Society of China
www.tnmsc.cn

Full shape memory effect of Cu−13.5Al−4Ni−6Fe shape memory martensite single crystal

Li-peng GUO[1,2], Jin-ping ZHANG[1,2], Xiao-qiang CHEN[1,2], Shi-wei ZHENG[1,2], Shui-yuan YANG[1,2], Shu-liang WANG[3], Jing-jing RUAN[4], Cui-ping WANG[2]

1. Fujian Key Laboratory of Materials Genome, College of Materials, Xiamen University, Xiamen 361005, China;
2. Shenzhen Research Institute of Xiamen University, Shenzhen 518000, China;
3. School of New Energy and Materials, Southwest Petroleum University, Chengdu 610500, China;
4. Institute for Advanced Studies in Precision Materials, Yantai University, Yantai 264005, China

Received 30 October 2021; accepted 1 March 2022

Abstract: The Cu−13.5Al−4Ni−6Fe centimeter-leveled martensite single crystals with full shape memory effect were prepared through simply annealing the cast alloy. The microstructure, reversible martensitic transformation, shape memory effect of this single crystal were investigated using optical microscopy, transmission electron microscope, differential scanning calorimeter, thermal mechanical analysis and compression test. The results show that Cu−13.5Al−4Ni−6Fe single crystal consists of 18R and 2H martensite, as well as rich-Fe bcc nanoprecipitate. The starting temperatures and the finishing temperatures of the forward and reverse martensitic transformations are 387, 397, 365 and 432 K, respectively. When the pre-strain is 6%, 7%, and 8%, this single crystal exhibits full shape memory effect of 4.4%, 4.7% and 5.2%, respectively. The obtained Cu−13.5Al−4Ni−6Fe martensite single crystal possesses shape memory properties that can be comparable to those of traditional shape memory alloys.

Key words: Cu−Al−Ni alloy; martensite single crystal; full shape memory effect; martensitic transformation; nanoprecipitate

1 Introduction

Shape memory alloys (SMAs) are a kind of functional materials which have thermoelastic martensitic transformation [1]. Their salient features are the shape memory effect (SME) and superelasticity (SE) [2]. The SME refers to the state in which the alloy can be stably deformed after being subjected to external forces. After being stimulated by temperature or magnetic field, the process of recovering deformed the state [2]. The residual strain disappears completely and the deformed alloy returns to its original shape, namely this is the full SME with 100% of shape recovery rate. In practical applications, a large and full SME is more advantageous.

Among all SMAs, the NiTi SMAs are the most widely used because they have not only good biocompatibility, but also great SE and SME [3]. However, the cytotoxicity and hypersensitivity of Ni have been reported in recent years, up to now, Ni substitution with β-Ti stabilizer elements (Ni free SMAs) has been studied [4−6]. Generally, for the most practically used NiTi SMAs, their martensitic transformation temperatures are relatively low, at the same time, their cost is higher than that of other SMAs [7,8]. In fact, the Cu-based SMAs are low cost, about one-tenth that of NiTi alloys, meanwhile, it has good cold workability and excellent conductivity of heat and electricity, therefore, they are increasingly favored by researchers, such as Cu−Al−Mn [9,10], Cu−Al−Ni [11,12], and Cu−Zn−Al SMAs [13]. Compared with other Cu-based

Corresponding author: Shui-yuan YANG, Tel: +86-18059243800, E-mail: yangshuiyuan@xmu.edu.cn;
Jing-jing RUAN, Tel: +86-18805929525, E-mail: ruanjingjingtohoku@163.com
DOI: 10.1016/S1003-6326(23)66195-3

SMAs, the Cu−Al−Ni SMAs are considered to have higher thermal stability and superior conductivity at operation temperature, at same time, the Cu−Al−Ni SMAs have higher martensitic transformation temperature [14]. However, their polycrystalline brittleness severely limits the production and processing of alloys [15−18]. Compared with polycrystalline alloys, the shape memory single crystal alloys usually have better mechanical and functional properties. But so far, single crystal alloys are usually obtained by special equipment and preparation processes, such as directional solidification (Bridgman and Czochralski methods) [19]. Recently, KUSAMA et al [20] prepared Cu−Al−Mn single crystal bar over 70 cm, it is mainly through the cyclic heat treatment in two different phase regions to induce sub-grain boundaries to prepare single crystals. This cyclic heat treatment process requires very strict conditions (heating and cooling rates, heating time, number of thermal cycles etc.), which are not conducive to practical production and application.

Recently, our research group reported a novel and simple method to prepare the Cu-based shape memory single crystal. In the Cu−Al−Mn alloy system, by adding the fourth component (Fe, Mo, V, Cr or W), an austenite single crystal can be obtained through only one annealing, and the single crystal has good superelasticity. Further research found that the fourth component plays a vital role in the system. It induces abnormal grain growth of the Cu−Al−Mn alloys and the production of centimeter-leveled single crystals [21−25]. Since such a result was found in the Cu−Al−Mn system, we speculate that the same phenomenon also exists in the Cu−Al−Ni alloy. So, in this work, the fourth component Fe element was added to the Cu−Al−Ni alloys with higher martensitic transformation temperature to obtain martensite single crystal. The microstructure, reversible martensitic transformation behaviors and shape memory properties were studied. This has certain guiding significance for the preparation of Cu-based shape memory single crystal alloys with full SME.

2 Experimental

2.1 Sample preparation

According to the mass fraction of Cu−13.5Al−4Ni−6Fe alloy, four pure components include copper (99.99%), aluminum (99.99%), nickel (99.99%) and iron (99.99%) were melted through the use of non-consumable tungsten electrodes at high arc under pure argon atmosphere. Ingot about 50 g was smelted repeatedly 5 times to ensure sufficiently uniform. Then it was cut to obtain a long sample about 5 mm thickness, followed by encapsulating in a quartz stone tube filled with argon gas. The sample was annealed at 1273 K for 24 h followed by quenching into water. The sample used for the SME test was obtained from the abnormally grown crystal grain, and the size was *d*3 mm × 5 mm.

2.2 Characterization of sample

After grinding and polishing, the sample was etched by a composition of 10 g $FeCl_3$ + 25 mL HCl + 100 mL H_2O etching solution. The macroscopic morphology was observed by an optical camera. The microstructure was observed by optical microscope and transmission electron microscope (TEM). The chemical composition analysis and composition mapping analysis of each element were determined by transmission electron microscopy-energy dispersive spectrometer (TEM-EDS). The martensitic transformation temperatures were determined by differential scanning calorimetry (DSC) at a heating and cooling rate of 10 K/min. The temperature range of DSC analyses was from 340 to 473 K. The SME of the alloy was characterized by the stress−strain curve and thermal mechanical analysis (TMA). The height of the sample was measured before loading (h_0) and after unloading (h_1). The SME was measured by TMA under an argon atmosphere at a heating and cooling rate of 10 K/min. The height was donated as (h_2) after the measurement of TMA. The residual strain (ε_r), SME strain (ε_{SME}) and SME rate (R_{SME}) were calculated as $\varepsilon_r=(h_0-h_1)/h_0\times100\%$, $\varepsilon_{SME}=(h_2-h_1)/h_0\times100\%$ and $R_{SME}=\varepsilon_{SME}/\varepsilon_r\times100\%$, respectively.

3 Results and discussion

3.1 Microstructure

Figure 1 shows the macroscopic morphology of the studied alloy before and after annealing at 1273 K for 24 h followed by water quenching. As a result, large grains and single crystals over centimeter-scale were obtained. At the same time, it

can be seen that both the cast and quenched alloys are martensite. This abnormal grain growth phenomenon is similar to the previously reported Cu−Al−Mn−(Fe, Mo, V, Cr or W) alloys [21−25].

As shown in Figs. 2 and 3, there are many fine nanoprecipitates existed besides the martensite both in the cast and single crystal. It can be seen that the nanoprecipitates are rich-Fe and poor-Cu. This result is consistent with that of the reported Cu−Al−Mn−Fe single crystals. In addition, the content and size of these nanoprecipitates of single crystal obviously decreased compared to the cast alloy. The shape of nanoprecipitates (NP) also changed from square to irregular small particles. The results of subsequent TEM test and the previous Cu−Al−Mn−Fe alloys confirm that these nanoprecipitates are bcc β(FeAl) phase.

In Figs. 4(a−f), it is found that the cast alloy consisted of fine square β(FeAl) nanoprecipitates and 2H martensite with typical twin structure. After quenching, there are different martensitic variants in Figs. 5(a−f) in which the 18R martensite was also observed. It has been confirmed that 2H and 18R martensites often coexist in Cu-based

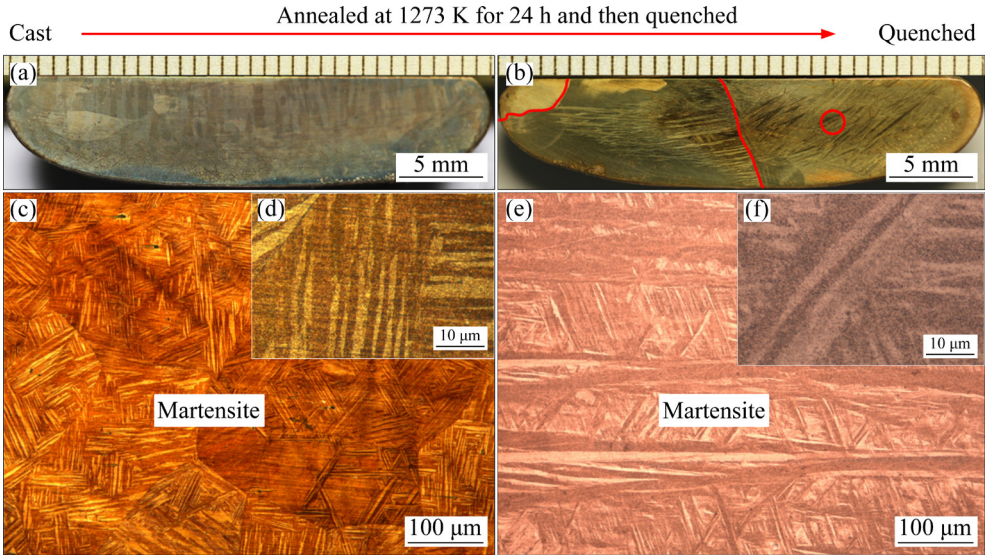

Fig. 1 Macroscopic morphologies of Cu−13.5Al−4Ni−6Fe cast alloy before and after annealing at 1273 K for 24 h (a, b), and optical micrographs of cast alloy (c, d) and single crystal (e, f)

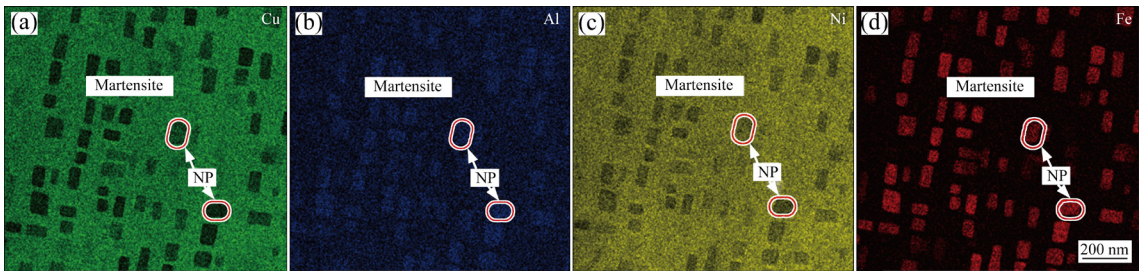

Fig. 2 Composition mapping analysis of Cu−13.5Al−4Ni−6Fe cast alloys

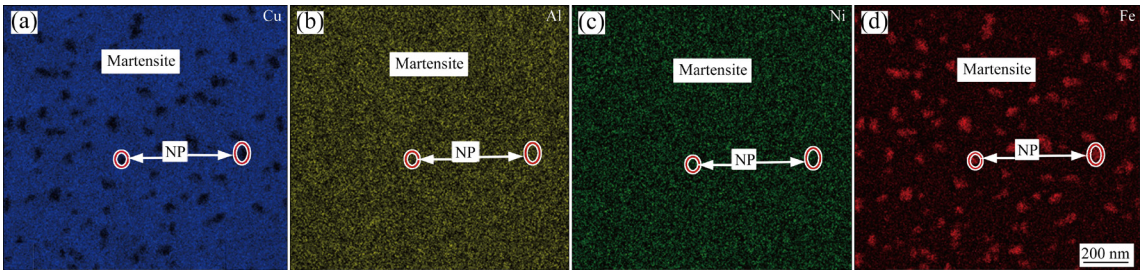

Fig. 3 Composition mapping analysis of Cu−13.5Al−4Ni−6Fe single crystal

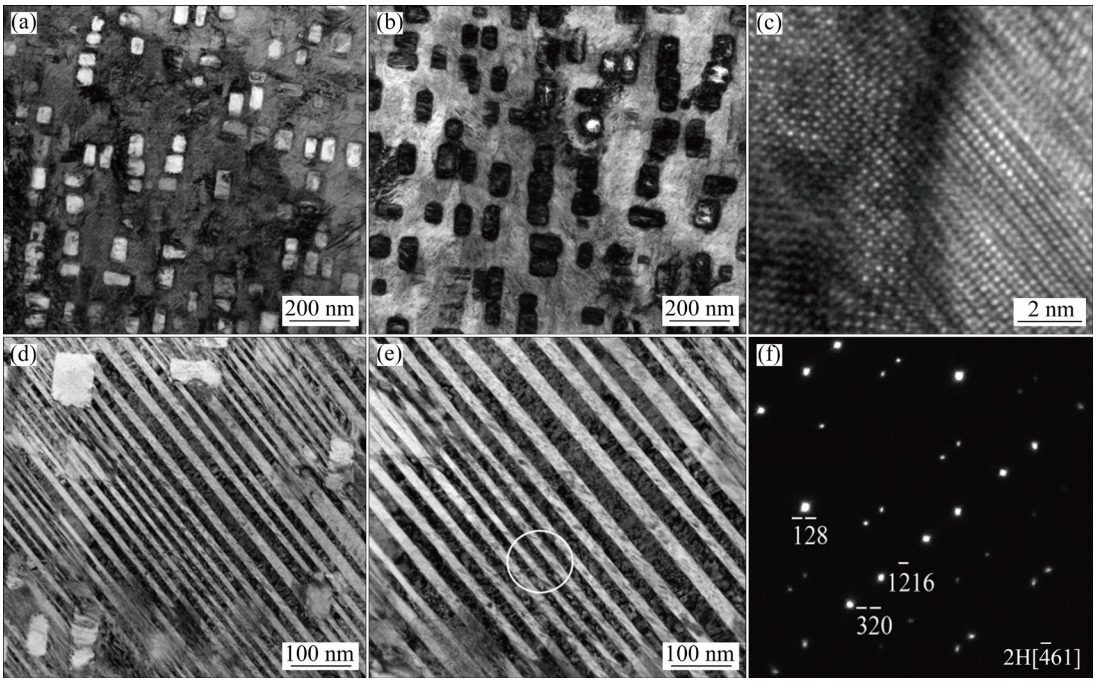

Fig. 4 Microstructure of Cu−13.5Al−4Ni−6Fe cast alloy: (a, d, e) TEM dark-field images; (b) TEM bright-field images; (c) High-angle annular dark-field scanning transmission electron microscopy (HAADF-STEM) image of two-phase region; (f) Selected area diffraction pattern of 2H martensite phase

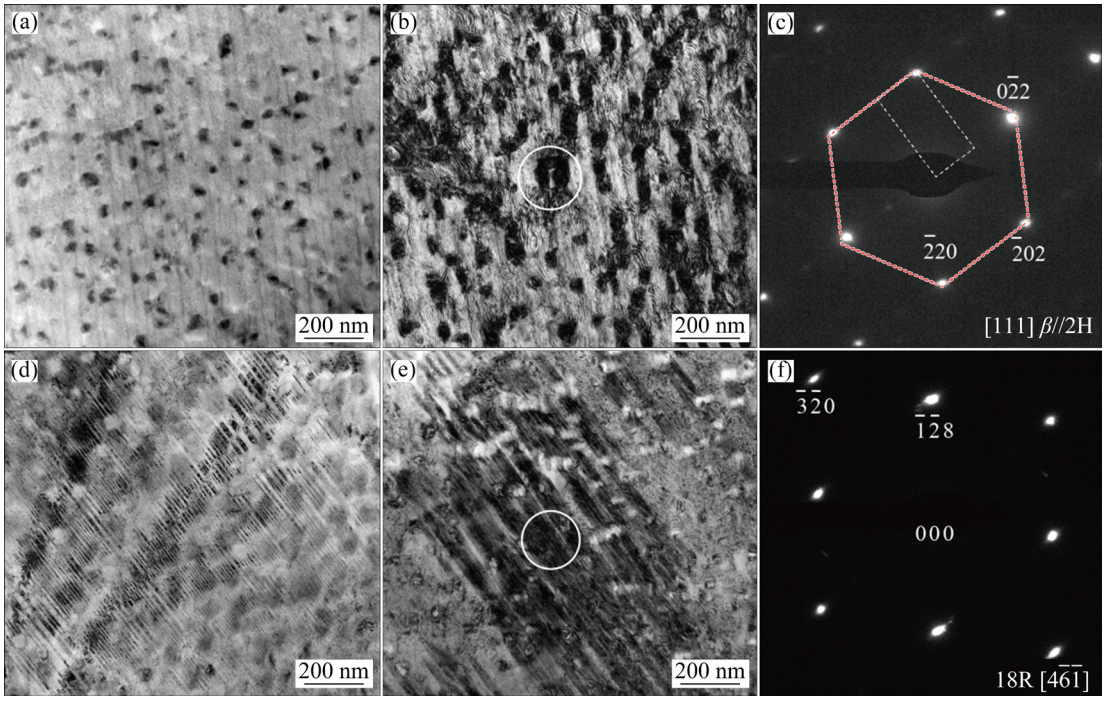

Fig. 5 Microstructure of Cu−13.5Al−4Ni−6Fe single crystal: (a, b, d) TEM bright-field images; (e) TEM dark-field images; (c) Selected area diffraction pattern of 2H martensite and β phase; (f) Selected area diffraction pattern of 18R martensite phase

SMAs [26,27]. Through the high-angle circular dark-field scanning transmission electron microscope analysis of single crystal, as shown in Fig. 5(c), it can be found that the martensite and the β(FeAl) phase are in a coherent relationship. The phenomenon is consistent with those results obtained in the Cu−Al−Mn−(Fe, Mo, V, Cr, or W) single crystals [21−25].

The phenomenon of abnormal grain growth exists while annealing some alloys with nano-precipitates, such as Fe−Si steel and Cu−Al binary alloy. In this study, the β(FeAl) nanoprecipitates play a very important role. Firstly, since the cast alloy is obtained by high-temperature melting and cooling, the low cooling rate causes a large number of β(FeAl) nanoprecipitates to be produced inside, and these nanoprecipitates will inhibit the growth of crystal grains during the crystallization process. Secondly, when the cast alloy is annealed at high enough temperature, these β(FeAl) nanoprecipitates will solid-dissolved back to the matrix (our previous results have confirmed this process in production process of Cu−Al−Mn−Fe and Cu−Al−Mn−Mo single crystals [21,22]). The dissolution process of β(FeAl) nanoprecipitates weakens the pinning effect on the grain boundary and releases a part of the energy. Then some grains with the preferred orientation will abnormally expand and extend until they cannot continue to grow. Thirdly, similar to the abnormal growth of Cu−Al−Mn−(Fe, Mo, V, Cr and W) alloys, the dissolution process of β(FeAl) nanoprecipitates also results in a microstructural change (orientation difference [28]) of Cu−Al−Ni−Fe alloy. The mechanism of abnormal grain growth of the present Cu−Al−Ni−Fe alloy is consistent with those of the previously reported Cu−Al−Mn−(Fe, Mo, V, Cr or W) alloys, which is not described here.

3.2 Martensite transformation

Figure 6 shows the DSC curve of the single crystal measured under a heating and cooling rate of 10 K/min. Obvious reversible martensitic transformation can be observed in the curve. The forward martensitic starting (M_s) and finishing (M_f) temperature are 387 and 365 K, respectively. The reverse martensitic starting (A_s) and finishing (A_f) temperature are 397 and 432 K, respectively.

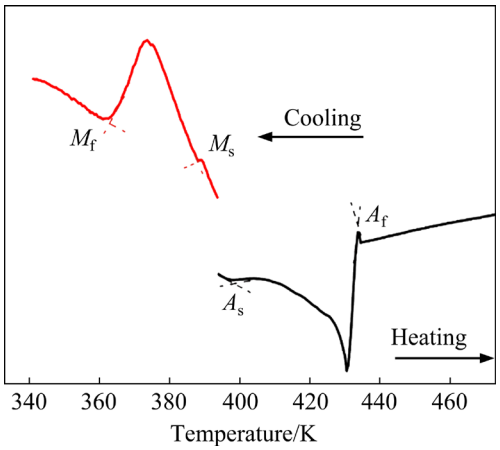

Fig. 6 DSC curve of Cu−13.5Al−4Ni−6Fe single crystal

3.3 Shape memory effect

The cylindrical single crystal specimens with a diameter of 3 mm and a height of 5 mm were cut from the abnormal grains, as shown by the circle on the right in Fig. 1. The specimens were deformed to different pre-strains of 6%, 7% and 8%, at the same time, unload to a zero-stress condition at room temperature. Figures 7(a, c, e) show the stress−strain curves when the alloy was compressed to 6%, 7% and 8%, respectively. When the sample was deformed by 6%, 7% and 8%, the residual strain was 4.4%, 4.7% and 5.2% respectively. After unloading, the deformed samples were heated to 573 K for 10 min for shape recovery by using TMA tests. The result was provided in Figs. 7(b, d, f). It is found that the residual strain of all specimens can be recovered completely. These results indicated that the obtained Cu−13.5Al−4Ni−6Fe single crystal exhibits excellent full shape memory effect. The largest SME is up to 5.2%, which is compared to those of conventional shape memory alloys [29−31].

It is well known that the single crystal orientation has a great influence on the performance of the single crystal. HORIKAWA et al [32] systematically studied the orientation dependence of $\beta_1 \rightarrow \beta_1'$ stress-induced martensite in the Cu−Al−Ni system; OMORI et al [33] also studied the relationship between stress hysteresis, superelastic behavior and orientation in the Cu−Al−Mn alloy system. In this study, the prepared Cu−13.5Al−4Ni−6Fe single crystal alloy exhibits martensite structure. When deforming this martensite single crystal at room temperature, generally the multiple variants of martensite reorientation or detwinning will occur, a residual strain is obtained after unloading. Then the residual strain would recover through heating above reverse martensitic transformation temperature. It can also be seen that as the stress becomes larger, the martensite reorientation platform will become more obvious, even when the pre-strain is 8%, a large stress platform will appear. At the same time, an instantaneous shape recovery behavior was observed, as shown in Fig. 7(f). This is mainly due to the disappearance of the resistance for inverse

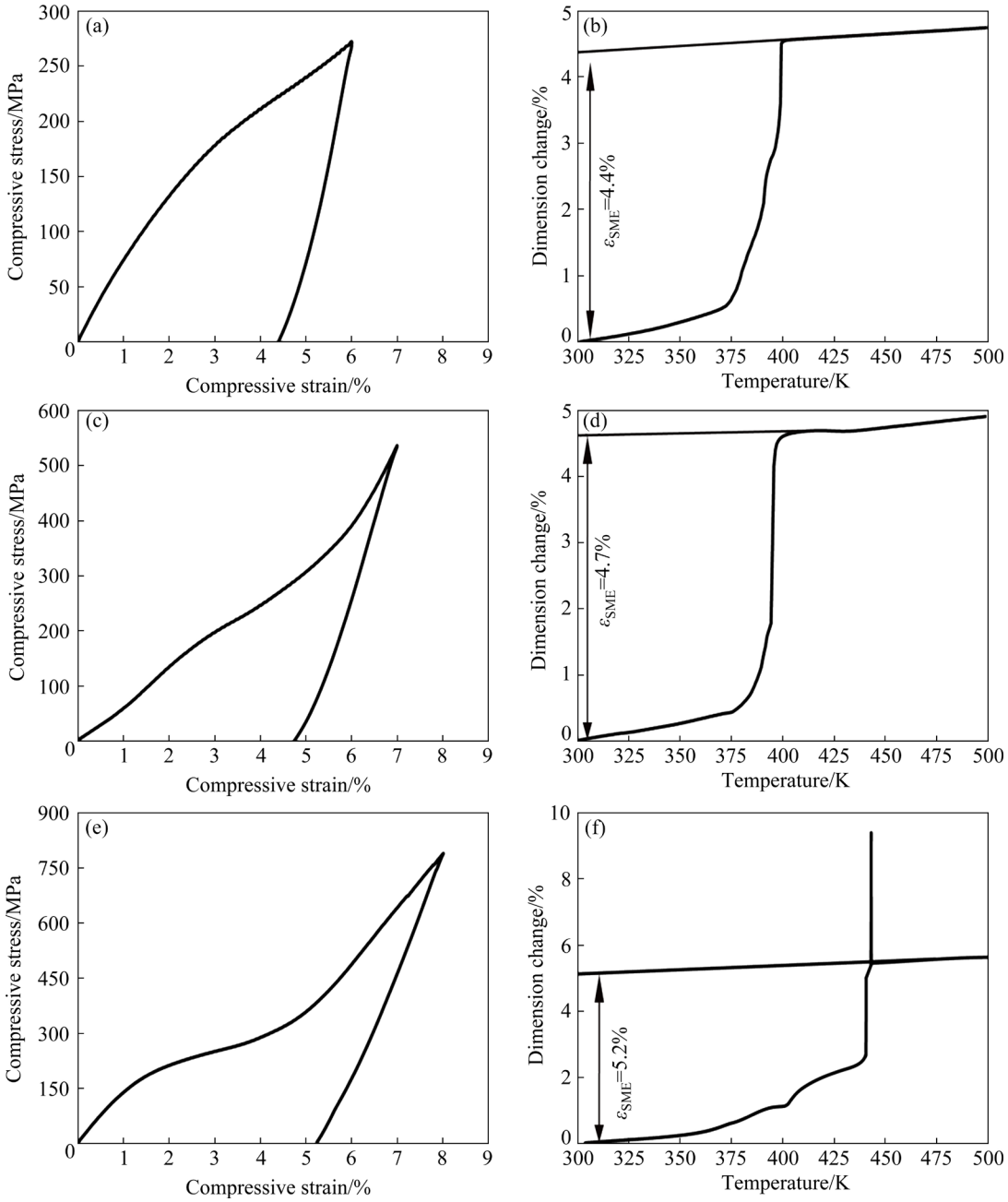

Fig. 7 Stress−strain curves (a, c, e) and TMA curves (b, d, f) of Cu−13.5Al−4Ni−6Fe martensite single crystals: (a, b) Pre-strain of 6%; (c, d) Pre-strain of 7%; (e, f) Pre-strain of 8%

martensitic transformation during heating, in which the resistance resulted from the nanoprecipitates. Similar results have been found in Cu−Al−Mn−Fe single crystal [23,28]. On the contrary, at low stress, the re-orientation of martensite is not very significant, so it appears as non-instantaneous recovery in the TMA curve. However, the stress-induced martensitic transformation process in the present study has not been studied in depth. The effect of multiple variants of martensite reorientation on the SME properties of Cu−13.5Al−4Ni−6Fe single crystal should be investigated in the future work.

4 Conclusions

(1) The Cu−13.5Al−4Ni−6Fe shape memory martensite single crystal over centimeter scale can be simply obtained while directly annealing the cast alloy at 1273 K for 24 h.

(2) The Cu−13.5Al−4Ni−6Fe shape memory martensite single crystal consists of 2H and 18R

martensite, as well as the β(FeAl) nanoprecipitates. The reversible martensitic temperatures of the single crystal are 387 K (M_s), 365 K (M_f), 397 K (A_s), 432 K (A_f), respectively.

(3) The Cu−13.5Al−4Ni−6Fe shape memory martensite single crystal has performance comparable to traditional shape memory alloy, in which full shape recovery characteristics can be obtained all the time while changing the deformation from 6%, to 7% and to 8%. The maximum recoverable strain is up to 5.2% with a recovery rate of 100%.

Acknowledgments

This work was supported by the financial supports from the Shenzhen Science and Technology Project, China (No. JCYJ20190809162401686), and the Guangdong Basic and Applied Basic Research Foundation, China (No. 2020A1515010069).

References

[1] ŌTSUKA K, WAYMAN C M. Shape memory materials [M]. Cambridge: Cambridge University Press, 1998.

[2] OTSUKA K, REN X B. Recent developments in the research of shape memory alloys [J]. Intermetallics, 1999, 7(5): 511−528.

[3] van HUMBEECK J. Non-medical applications of shape memory alloys [J]. Materials Science and Engineering: A, 1999, 273/274/275: 134−148.

[4] BAHADOR A, HAMZAH E, KONDOH K, ASMA ABUBAKAR T, YUSOF F, UMEDA J, SAUD S N, IBRAHIM M K. Microstructure and superelastic properties of free forged Ti−Ni shape-memory alloy [J]. Transactions of Nonferrous Metals Society of China, 2018, 28(3): 502−514.

[5] BAHADOR A, HAMZAH E, KONDOH K, ABU BAKAR T A, YUSOF F, IMAI H, SAUD S N, IBRAHIM M K. Effect of deformation on the microstructure, transformation temperature and superelasticity of Ti−23at.%Nb shape-memory alloys [J]. Materials & Design, 2017, 118: 152−162.

[6] IBRAHIM M K, HAMZAH E, SAUD S N, NAZIM E M, IQBAL N, BAHADOR A. Effect of Sn additions on the microstructure, mechanical properties, corrosion and bioactivity behaviour of biomedical Ti−Ta shape memory alloys [J]. Journal of Thermal Analysis and Calorimetry, 2018, 131(2): 1165−1175.

[7] HEDAYAT I, DEZFULI F, ALAM M S. Performance-based assessment and design of FRP based high damping rubber bearing incorporated with shape memory alloy wires [J]. Engineering Structures, 2014, 61: 166−183.

[8] ZHANG Yun-feng, CAMILLERI J A, ZHU Song-ye. Mechanical properties of superelastic Cu−Al−Be wires at cold temperatures for the seismic protection of bridges [J]. Smart Materials and Structures, 2008, 17(2): 025008.

[9] LIU Ji-li, HUANG Hai-you, XIE Jian-xin. Superelastic anisotropy characteristics of columnar grained Cu−Al−Mn shape memory alloys and its potential applications [J]. Materials & Design, 2015, 85: 211−220.

[10] OLIVEIRA J P, PANTON B, ZENG Z, OMORI T, ZHOU Y, MIRANDA R M, BRAZ FERNANDES F M. Laser welded superelastic Cu−Al−Mn shape memory alloy wires [J]. Materials & Design, 2016, 90: 122−128.

[11] NAKATA Y, TADAKI T, SHIMIZU K. Thermal cycling effects in a Cu−Al−Ni shape memory alloy [J]. Transactions of the Japan Institute of Metals, 1985, 26(9): 646−652.

[12] MATLAKHOVA L A, PEREIRA E C, MATLAKHOV A N, MONTEIRO S N, TOLEDO R. Mechanical behavior and fracture characterization of a monocrystalline Cu−Al−Ni subjected to thermal cycling treatments under load [J]. Materials Characterization, 2008, 59(11): 1630−1637.

[13] BONNOT E, ROMERO R, MORIN M, VIVES E, MAÑOSA L, PLANES A. In-situ observations of a martensitic transformation in a Cu−Zn−Al single crystal driven by stress or strain [J]. Journal of Materials Science, 2008, 43(11): 3832−3836.

[14] YANG, Shui-yuan, SU Yu, WANG Cui-ping, LIU Xin-jun. Microstructure and properties of Cu−Al−Fe high-temperature shape memory alloys [J]. Materials Science and Engineering: B, 2014, 185: 67−73.

[15] SAKAMOTO H, SHIMIZU K, OTSUKA K. Fatigue properties associated with cyclic $\beta_1 \rightleftharpoons \beta_1'$ transformation pseudoelasticity of Cu−Al−Ni alloy single crystals [J]. Transactions of the Japan Institute of Metals, 1981, 22(8): 579−587.

[16] SAKAMOTO H, KIJIMA Y, SHIMIZU K, OTSUKA K. Twinning pseudoelasticity caused by cyclic stress in a single crystal Cu−Al−Ni alloy [J]. Scripta Metallurgica, 1981, 15(3): 281−285.

[17] CREUZIGER A, CRONE W C. Grain boundary fracture in CuAlNi shape memory alloys [J]. Materials Science and Engineering: A, 2008, 498(1/2): 404−411.

[18] PEREIRA E C, MATLAKHOVA L A, MATLAKHOV A N, de ARAÚJO C J, SHIGUE C Y, MONTEIRO S N. Reversible martensite transformations in thermal cycled polycrystalline Cu−13.7%Al−4.0%Ni alloy [J]. Journal of Alloys and Compounds, 2016, 688: 436−446.

[19] MORÁN M J, CONDÓ A M, HABERKORN N. Recrystallization and martensitic transformation in nanometric grain size Cu−Al−Ni thin films grown by DC sputtering at room temperature [J]. Materials Characterization, 2018, 139: 446−451.

[20] KUSAMA T, OMORI T, SAITO T, KISE S, TANAKA T, ARAKI Y, KAINUMA R. Ultra-large single crystals by abnormal grain growth [J]. Nature Communications, 2017, 8(1): 1−9.

[21] YANG Shui-yuan, OMORI T, WANG Cui-ping, LIU Yong, NAGASAKO M, RUAN Jing-jing, KAINUMA R, ISHIDA K, LIU Xing-jun. A jumping shape memory alloy under heat [J]. Scientific Reports, 2016, 6(1): 1−6.

[22] YANG Shui-yuan, ZHANG Ji-xun, CHI Meng-yuan, WEN Yu-hua, WANG Cui-ping, LIU Xing-jun. Low-cost Cu-based shape memory single crystals obtained by abnormal grain growth showing excellent superelasticity [J]. Materialia, 2019, 5: 100200.

[23] YANG Shui-yuan, CHI Meng-yuan, ZHANG Ji-xun, LU Yong, HUANG Yi-xiong, WANG Cui-ping, LIU Xing-jun. Abnormal grain growth in annealing cast Cu−Al−Mn−V alloys and their superelasticity [J]. Smart Materials and Structures, 2019, 28(5): 055015.
[24] YANG Shui-yuan, ZHANG Ji-xun, CHI Meng-yuan, YANG Mu-jin, WANG Cui-ping, LIU Xing-jun. Excellent superelasticity of Cu−Al−Mn−Cr shape memory single crystal obtained only through annealing cast polycrystalline alloy [J]. Scripta Materialia, 2019, 165: 20−24.
[25] YANG Shui-yuan, ZHANG Ji-xun, CHEN Xin-ren, CHI Meng-yuan, WANG Cui-ping, LIU Xing-jun. Excellent superelasticity and fatigue resistance of Cu−Al−Mn−W shape memory single crystal obtained only through annealing polycrystalline cast alloy [J]. Materials Science and Engineering: A, 2019, 749: 249−254.
[26] PICORNELL C, PONS J, CESARI E. Stress−temperature relationship in Cu−Al−Ni single crystals in compression mode [J]. Materials Science and Engineering: A, 2004, 378(1/2): 222−226.
[27] SARI U, AKSOY İ. Electron microscopy study of 2H and 18R martensites in Cu−11.92wt.%Al−3.78wt.%Ni shape memory alloy [J]. Journal of Alloys and Compounds, 2006, 417(1/2): 138−142.
[28] YANG Shui-yuan, QING Xin-yu, ZHANG Ji-xun, GUO Li-peng, HONG Shen, LI Ming-pei, ZHANG Jin-bin, WANG Cui-ping, LIU Xing-jun. Role of β(FeAl) nanoparticles in abnormal grain growth in the annealing of cast Cu−Al−Mn−Fe shape memory alloys [J]. Progress in Natural Science: Materials International, 2020, 30(4): 510−516.
[29] ZHANG Xin, SUI Jie-he, LIU Qing-suo, CAI Wei. Effects of Gd addition on the microstructure, mechanical properties and shape memory effect of polycrystalline Cu−Al−Ni shape memory alloy [J]. Materials Letters, 2016(180): 223−227.
[30] ZHANG Xin, LIU Qing-suo. Influence of alloying element addition on Cu−Al−Ni high temperature shape memory alloy without second phase formation [J]. Acta Metallurgica Sinica, 2016, 29(9): 884−888.
[31] ZHANG Xin, CUI Tian-yu, LIU Qing-suo, DONG Zhi-zhong, MAN Cheng. Effect of Nd addition on the microstructure, mechanical properties, shape memory effect and corrosion behavior of Cu−Al−Ni high temperature shape memory alloys [J]. Journal of Alloys and Compounds, 2021, 858: 157685.
[32] HORIKAWA H, ICHINOSE S, MORII K, MIYAZAKI S, OTSUKA K. Orientation dependence of $\beta_1 \rightarrow \beta'_1$ stress-induced martensitic transformation in a Cu−Al−Ni alloy [J]. Metallurgical and Materials Transactions: A, 1988, 19(4): 915−923.
[33] OMORI T, KAWATA S, KAINUMA R. Orientation dependence of superelasticity and stress hysteresis in Cu−Al−Mn alloy [J]. Materials Transactions, 2020, 61(1): 55−60.

具有完全形状记忆效应的 Cu−13.5Al−4Ni−6Fe 形状记忆马氏体单晶

郭利鹏[1,2]，张锦平[1,2]，陈晓强[1,2]，郑师威[1,2]，杨水源[1,2]，王书亮[3]，阮晶晶[4]，王翠萍[2]

1. 厦门大学 材料学院，福建省材料基因重点实验室，厦门 361005；
2. 厦门大学 深圳研究院，深圳 518000；
3. 西南石油大学 新能源与材料学院，成都 610500；
4. 烟台大学 精准材料高等研究院，烟台 264005

摘 要：通过对铸态合金进行简单退火处理，制备具有完全形状记忆效应的厘米级 Cu−13.5Al−4Ni−6Fe 马氏体单晶。通过光学显微镜、透射电子显微镜、差示扫描量热仪、热机械分析仪以及压缩测试研究单晶的显微组织、逆马氏体转变和形状记忆效应。研究结果表明，Cu−13.5Al−4Ni−6Fe 单晶拥有 18R 和 2H 2 种马氏体，同时拥有体心立方富 Fe 纳米析出相。马氏体转变和逆转变的起始温度和结束温度分别为 387、397、365 和 432 K。当对单晶施加 6%、7%以及 8%的预应变时，单晶分别拥有 4.4%、4.7%以及 5.2%的完全形状记忆效应。获得的 Cu−13.5Al−4Ni−6Fe 马氏体单晶具有可与传统形状记忆合金相媲美的形状记忆性能。

关键词：Cu−Al−Ni；马氏体单晶；完全形状记忆效应；马氏体转变；纳米析出相

(Edited by Xiang-qun LI)